Chemical Physics Letters 554 (2012) 243–247

Contents lists available at SciVerse ScienceDirect

Chemical Physics Letters

journal homepage: www.elsevier.com/locate/cplett

Local vibrational modes of the water dimer – Comparison of theory and experiment

R. Kalescky, W. Zou, E. Kraka, D. Cremer *

Department of Chemistry, Southern Methodist University, 3215 Daniel Avenue, Dallas, TX 75275, United States

ARTICLE INFO

Article history:
Received 3 September 2012
In final form 17 October 2012
Available online 24 October 2012

ABSTRACT

Local and normal vibrational modes of the water dimer are calculated at the CCSD(T)/CBS level of theory. The local H-bond stretching frequency is 528 cm^{-1} compared to a normal mode stretching frequency of just 143 cm^{-1}. The adiabatic connection scheme between local and normal vibrational modes reveals that the lowering is due to mass coupling, a change in the anharmonicity, and coupling with the local HOH bending modes. The local mode stretching force constant is related to the strength of the H-bond whereas the normal mode stretching force constant and frequency lead to an erroneous underestimation of the H-bond strength.

1. Introduction

The water dimer (**1**) gains its stability from H-bonding between the monomers [1,2]. Because H-bonding in **1** is considered as prototypical and affects many of the properties of liquid water, it has been numerously investigated utilizing both experimental and computational means [1,2]. In a recent investigation, Freindorf, Kraka, and Cremer (FKC) [3] investigated H-bonding with the help of local vibrational modes as they were first defined by Konkoli and Cremer [4]. They determined the relative strength of 65 different H-bonds via the local mode stretching force constants. An important result of their work is that the local mode H-bond stretching frequencies appear in the region 300–600 cm^{-1}, i.e. significantly above those values, which have been determined so far for H-bond stretching frequencies [5–7]. This in itself is not necessarily a contradiction because FKC considered harmonic rather than anharmonically corrected vibrational frequencies, where the latter being better comparable with measured vibrational frequencies. H-bonding is known to lead to large anharmonic corrections [8], which may directly or indirectly cause the large difference between harmonic and anharmonic vibrational frequencies.

In this Letter, we will determine normal and local vibrational modes for the H-bond stretching of the water dimer, discuss how anharmonicity effects change their relationship, and draw conclusions with regard to the energetic implications of H-bonding. In addition, we characterize all 12 normal vibrational modes of **1** in terms of local vibrational modes to be able to derive typical OH and O···H vibrational frequencies and force constants. Our investigation is based on high level ab initio calculations of the CCSD(T)-type to obtain sets of reliable normal and local vibrational frequencies for **1**.

2. Computational methods

By solving the Euler–Lagrange equations, one can derive the eigenvalue problem of vibrational spectroscopy and express it in the following matrix form [9]

$$\mathbf{F}^q\mathbf{D} = \mathbf{G}^{-1}\mathbf{D}\mathbf{\Lambda} \tag{1}$$

where $\mathbf{F}^q$ is the force constant matrix expressed in internal coordinates q_n, $\mathbf{D}$ collects the vibrational eigenvectors $\mathbf{d}_\mu$ in form of column vectors ($\mu = 1,\ldots,N_{vib}$ with $N_{vib} = 3N - L$; N: number of atoms; L: number of translations and rotations), $\mathbf{G}$ is the Wilson G-matrix [9] and $\mathbf{\Lambda}$ is a diagonal matrix containing the vibrational eigenvalues $\lambda_\mu = 4\pi^2c^2\omega_\mu^2$ where ω_μ represents the (harmonic) vibrational frequency of mode $\mathbf{d}_\mu$.

Konkoli and Cremer have defined local vibrational modes by solving mass-decoupled Euler–Lagrange equations [4]. A local mode $\mathbf{a}_n$ obtained in this way is associated with an internal coordinate q_n leading the mode. Mode vector $\mathbf{a}_n$ takes the form [4]:

$$\mathbf{a}_n = \frac{\mathbf{K}^{-1}\mathbf{d}_n^\dagger}{\mathbf{d}_n\mathbf{K}^{-1}\mathbf{d}_n^\dagger} \tag{2}$$

where the (diagonal) force constant matrix $\mathbf{K}$ is given according to [3,4,10]:

$$\mathbf{K} = \mathbf{D}^\dagger\mathbf{F}^q\mathbf{D} \tag{3}$$

Note that $\mathbf{d}_n$ is now a row vector of matrix $\mathbf{D}$. The local mode force constant $k_{a,n}$ is given by Eq. (4):

$$k_{a,n} = \mathbf{a}_n^\dagger\mathbf{K}\mathbf{a}_n = (\mathbf{d}_n\mathbf{K}^{-1}\mathbf{d}_n^\dagger)^{-1} \tag{4}$$

Local mode force constants, contrary to normal mode force constants, have the advantage of being independent of the choice of the coordinates, which are used to describe the molecule in question. This relates them to the compliance constants Γ_i of Decius

* Corresponding author.
E-mail address: dieter.cremer@gmail.com (D. Cremer).

0009-2614/$ - see front matter © 2012 Published by Elsevier B.V.
http://dx.doi.org/10.1016/j.cplett.2012.10.047

[11] defined via the inverse force constant matrix both being expressed in terms of internal coordinate q:

$$\mathbf{\Gamma}^q = (\mathbf{F}^q)^{-1} = \mathbf{D}\mathbf{K}^{-1}\mathbf{D}^\dagger \tag{5}$$

which leads to

$$k_{a,n} = 1/(\mathbf{\Gamma}^q)_{nn} = 1/\Gamma_n \tag{6}$$

i.e., the compliance constants of Decius [11] can be simply derived from the local mode force constants of Konkoli and Cremer [4].

One can re-write the Wilson Eq. (1) with the help of the compliance matrix as:

$$\begin{aligned} &\mathbf{G}(\mathbf{\Gamma}^q)^{-1}\mathbf{D} = \mathbf{D}\mathbf{\Lambda} \\ &\mathbf{G}\mathbf{R} = \mathbf{\Gamma}^q\mathbf{R}\mathbf{\Lambda} \end{aligned} \tag{7}$$

where a new eigenvector matrix $\mathbf{R} = (\mathbf{\Gamma}^q)^{-1}\mathbf{D}$ is introduced. By partitioning matrices $\mathbf{\Gamma}^q$ and $\mathbf{G}$ into diagonal ($\mathbf{\Gamma}^q_d$ and $\mathbf{G}_d$) and off-diagonal ($\mathbf{\Gamma}^q_o$ and $\mathbf{G}_o$) parts and introducing the scaling factor λ ($0 \leqslant \lambda \leqslant 1$), Eq. (7) becomes

$$(\mathbf{G}_d + \lambda\mathbf{G}_o)\mathbf{R}_\lambda = (\mathbf{\Gamma}^q_d + \lambda\mathbf{\Gamma}^q_o)\mathbf{R}_\lambda\mathbf{\Lambda}_\lambda \tag{8}$$

[10] where $\mathbf{R}$ and $\mathbf{\Lambda}$ depend on λ. Eq. (8) is the basis for an adiabatic connection scheme, which relates local vibrational modes to normal vibrational modes in terms of their eigenvalues (frequencies) and eigenvectors (mode vectors) [10]. In this way, each normal mode frequency ω_μ can be expressed by a local mode frequency ω_a and a coupling frequency ω_c, i.e. $\omega_\mu = \omega_a + \omega_c$. The zero-point energy (ZPE) is split up in two parts where one results from the local mode frequencies and one from the coupling frequencies [10].

Equilibrium geometry, harmonic vibrational frequencies, and harmonic infrared intensities of the water dimer (see Figure 1) were calculated at the CCSD(T) level of theory [12] correcting for basis set superposition errors and using Dunning's aug-cc-pVDZ, aug-cc-pVTZ, and aug-cc-pVQZ basis sets. These calculations were the basis for extrapolating results to the complete basis set (CBS) limit. Employing CCSD(T)/aug-cc-VTZ, anharmonic corrections for frequencies and intensities were determined utilizing vibrational perturbation theory (VPT) at second order.[13,14] Independently, harmonic CBS frequencies were scaled using group scaling factors for covalent stretching (0.953), covalent bending (0.962), and non-covalent modes (0.873 and 0.705) as determined in this Letter. Local vibrational frequencies were calculated from normal vibrational frequencies [4]. Experimental local mode frequencies are calculated according to the procedure given by Cremer and co-workers [15]. The adiabatic connection scheme of Eq. (8) was used to relate local to normal mode frequencies and to determine coupling frequencies, which provide a cumulative measure for the strength of coupling between local modes. The normal vibrational modes are characterized in terms of local vibrational modes using the CNM (characterizing normal modes) approach by Konkoli and Cremer [16]. All coupled cluster calculations were carried out with the program CFOUR [17].

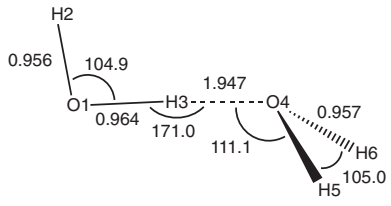

Figure 1. CCSD(T)/CBS geometry of the water dimer. Bond lengths in Å and angles in degrees. The numbering of atoms is used throughout of this Letter.

3. Results and discussion

In Figure 1, the CCSD(T)/CBS geometry of **1** is given, which compares well with the results of previous investigations [18]. The CCSD(T)/CBS H-bond binding energy is −5.0 kcal/mol corresponding to an enthalpy and free energy value at 298 K of −3.4 and 2.7 kcal/mol. Min and co-workers obtained binding energies of −5.01 ± 0.01 kcal/mol depending on what basis sets were used for the CBS limit calculation [18], which is in line with an earlier result of Klopper and co-workers [19]. Hence, the CCSD(T)/CBS results obtained in this Letter can be considered to be accurate. Noteworthy is that **1** is unstable under normal conditions due to a strong decrease of the entropy, which is in line with experimental measurements. For example, Curtiss and co-workers [20] studied dimers **1** at 373 K and found $\Delta G(373) = 3.3$ kcal/mol. At this temperature the mole fraction of **1** in water vapor is 0.011 [20]. All spectroscopic measurements of **1** have been carried out at reduced temperatures between 5 K and maximally 80 K under low pressure [21–25]. We obtain for 20 K and 3 Pa a free binding energy $\Delta G(20)$ of 2.0 kcal/mol thus confirming the stability of **1** under these conditions.

In Table 1, calculated harmonic and anharmonically corrected CCSD(T) vibrational frequencies are compared with the experimental frequencies of **1** [21–25]. The anharmonically corrected CCSD(T)/CBS frequencies compare well with the known experimental frequencies and have an average deviation of just 15.1 cm^{-1} where the largest deviations are found for the low frequencies, which are more difficult to measure [21–23]. Using group scaling an average deviation of just 7.1 cm^{-1} is achieved (see Table 1). Results are in line with other high-accuracy calculations of the frequencies of **1** [14].

In Table 2, each normal mode is decomposed into local vibrational modes. The corresponding local mode frequencies are given in Table 3 together with the corresponding coupling frequencies, which are taken from the adiabatic connection scheme of Figure 2a and b. The coupling of the local modes depends on the closeness of their frequencies, the degree of alignment of the mode vector, and the mass ratios of the atoms involved in a local mode. For example, the degeneracy of the stretching frequencies of the O4H5 and the O4H6 bonds ($\omega_a = 3694$ cm^{-1}) leads to large coupling and the formation of an asymmetric ($A''; \omega_\mu = 3763$ $cm^{-1}; \omega_c = 69$ cm^{-1}) and a symmetric normal mode ($A'; \omega_\mu = 3669$ $cm^{-1}; \omega_c = -25$ cm^{-1}). A typical mass-effect is found for the bending mode H2O1H3. If this is local it has a 63 cm^{-1} lower frequency (1590 cm^{-1}, Table 3) than H5O4H6 bending (1653 cm^{-1}; enhanced by anharmonicity effects to 93 cm^{-1}, i.e. 1511 vs. 1604 cm^{-1}, Table 3), which is due to the weakening of the O1H3 donor bond. In the normal mode, the mass effect of the second water molecule comes in and pushes the frequency $\omega_a(H_2O_1H_3)$ up by 89 cm^{-1} (anharmonically corrected by 113 cm^{-1}) causing in this way a diabatic avoided crossing with the H5O4H6 bending mode at $\lambda = 0.98$ and $\omega = 1619$ cm^{-1} (see Figure 2), The mode character is exchanged at the avoided crossing so that ω_8 rather than ω_7 becomes the H2O1H3 bending mode (the softer bend is on top of the stiffer bend; Table 2).

In a similar way, the changes in the frequency of the local H-bond stretching mode are effected. The effective mass of O4 increases in the normal mode due to the fact that O4 is bonded to H5 and H6, which leads to a lowering of the H3···O4 stretching frequency. This causes an adiabatic avoided crossing at $\lambda = 0.75$ (300 cm^{-1}) with the O1H3O4 bending mode accompanied by a switch in the mode character. The lower normal mode, $\mathbf{d}_4$, is now the H-bond stretching mode, however with a strong admixture of O1H3O4 bending character. Additional avoided crossings between the vibrational eigenstates of modes $\mathbf{d}_4$ and $\mathbf{d}_3$ as well as $\mathbf{d}_1$ lead to the admixture of H3O4H5 and H3O4H6 bending character and a large harmonic coupling frequency ω_c of 340 cm^{-1}.

Table 1
Harmonic normal mode frequencies ω_μ (in cm^{-1}) of the water dimer calculated using CCSD(T) and the aug-cc-pVXZ basis sets (X = D, T, and Q). These frequencies were used to calculate a CBS frequency for each mode. CCSD(T)/aug-cc-pVTZ anharmonic corrections (Anh. Corr.) were applied to get anharmonic CBS frequencies, $\omega_{CBS,Anh.}$. In the last row the mean deviation (m.d.) of calculated from measured frequencies is given.

#	Sym.	ω_μ (VDZ)	ω_μ (VTZ)	ω_μ (VQZ)	ω_μ (CBS)	Anh. Corr.	ω_μ(CBS, Anh.)	ω_μ (Scaled)	ω_μ (Exp.)
1	A''	130.7	134.9	131.3	129.2	−44.2	85.0	91	88 [21]
2	A''	148.4	148.0	149.0	149.6	−22.8	126.8	105	103 [21]
3	A'	146.7	151.9	154.6	156.1	−33.6	122.6	110	108 [21]
4	A'	184.9	190.7	189.2	188.3	−40.6	147.7	133	143 [22]
5	A'	357.3	372.3	358.2	349.8	−55.5	294.3	305	311 [23]
6	A''	634.6	649.5	625.1	610.6	−126.1	484.5	533	523 [23]
7	A'	1640.9	1643.3	1655.7	1663.0	−43.4	1619.6	1600	1599 [23]
8	A'	1659.7	1667.8	1674.3	1678.2	−53.8	1624.3	1615	1616 [23]
9	A'	3713.5	3756.4	3755.2	3754.3	−140.0	3614.3	3578	3601 [24]
10	A'	3784.1	3829.6	3836.4	3840.2	−171.7	3668.5	3660	3660 [24]
11	A'	3878.1	3911.2	3921.0	3926.8	−179.9	3746.9	3742	3735 [24]
12	A''	3897.9	3930.1	3941.9	3948.7	−186.0	3762.7	3763	3745 [25]
m.d.		78.7	96.1	96.7	96.9		15.1	7.1	

Table 2
Characterization of the normal modes ω_μ(CBS) of **1** in terms of the local mode contributions ω_a(CBS).

μ	Characterization of modes ω_μ(CBS) in terms of modes ω_a(CBS)
1	48.6% (H5–O4–H3 + H6–O4–H3), 35.1% H5–O4–H3–O_1, 16.2% H2–O1–H3–O4
2	40.4% H2–O1–H3–O4, 38.4% (H5–O4–H3 + H6–O4–H3), 21.1% H5–O4–H3–O1
3	37.7% O1–H3–H4, 30.6% (H5–O4–H3 + H6–O4–H3), 28.3% H3–O4
4	58.5% H3–O4, 20.1% O1–H3–H4, 19.8% (H5–O4–H3 + H6–O4–H3)
5	58.5% O1–H3–H4, 22.8% (H5–O4–H3 + H6–O4–H3), 17.4% H2–O1–H3
6	44.6% H2–O1–H3–O4, 38.5% H5–O4–H3–O1, 17.0% (H5–O4–H3 + H6–O4–H3)
7	94.0% H5–O4–H6
8	91.3% H2–O1–H3
9	85.2% O1–H3, 12.6% O1–H2
10	98.8% (O4–H5 + O4–H6)
11	86.9% O1–H2, 12.8% O1–H3
12	100.0% (O4–H5 + O4–H6)

Although the H-bond stretching character of mode $\mathbf{d}_4$ still dominates (59%, Table 2), it is problematic to draw from the frequency thus obtained any conclusions on the strength of the H-bond in **1**.

In addition to the local mode coupling, there is also a large anharmonicity effect of 108 cm^{-1} (from 528 to 420 cm^{-1}, see Table 3) for the local H-bond stretching mode. This effect is large compared to the 41 cm^{-1} anharmonicity correction of normal mode 4, however it is still small in comparison to the 173–179 cm^{-1} anharmonicity corrections for the local O1H2 and O4H5 stretching frequencies or the 145 cm^{-1} obtained for the local OH donor stretching frequency. As a result of the admixture of bending character the anharmonic character of H-bond stretching is reduced. We can confirm that the anharmonicity of the O1H3 donor stretching frequency changes, however it is reduced rather than increased when compared with the O1H2 and O4H5 (O4H6) stretching.

4. Conclusions

In this Letter, we have shown that the large difference between the local and normal H-bond stretching frequency (i.e. that frequency being associated with H-bond stretching) of **1** results from three different effects: (i) mass coupling due to the increase of the mass of the O4(H5H6) and the H3(O1H2) unit not contained in a local mode; (ii) a larger anharmonicity of the local mode (108 cm^{-1} compared to 41 cm^{-1} in the normal mode), and (iii) strong coupling with OH···O and H···OH bending modes. Our analysis reveals that the frequency measured at 143 cm^{-1} is associated with a mode that contains according to CCSD(T) calculations 58% H-bond stretching character and 40% bending character, where the latter contributions are in line with a large coupling frequency of 272.6 cm^{-1}. This leads to the important conclusion that a direct interpretation of H-bond stretching frequencies as descriptors of the strength of the H-bond is misleading because mass and coupling effects as well as the anharmonicity of the H-bond stretching

Table 3
Local mode frequencies ω_a, local force constant k_a, coupling frequencies ω_c, and zero-point-energies (ZPE) of **1**.

Type	ω_a(CBS) Harm. (cm^{-1})	ω_a(CBS) Anharm. (cm^{-1})	ω_a(Exp.) (cm^{-1})	k_a(Exp.) (mdyn $Å^{-1}$)[a]	ω_c(CBS) Harm. (cm^{-1})	ω_c(CBS) Anharm. (cm^{-1})	ω_c(Exp.) (cm^{-1})
ω_a(H6–O4–H3)	235.8	179.3	168.3	0.012	−106.6	−94.3	−83.3
ω_a(H5–O4–H3)	235.8	179.3	168.3	0.012	−86.2	−56.7	−45.7
ω_a(H5–O4–H3–O1)	322.8	237	231.2	0.000	−166.7	−110.2	−104.4
ω_a(H3–O4)	528.5	420.3	390.4	0.085	−340.2	−272.6	−242.7
ω_a(O1–H3–H4)	372.9	305.6	287.5	0.020	−23.1	−11.3	6.8
ω_a(H2–O1–H3–O4)	328.3	255.2	236.1	0.000	282.3	229.3	248.4
ω_a(H5–O4–H6)	1653	1604.4	1583.5	0.635	10.0	15.2	36.1
ω_a(H2–O1–H3)	1589.6	1511.1	1503.6	0.575	88.6	113.2	120.7
ω_a(O1–H3)	3764.9	3620	3606.9	7.267	−10.6	−5.7	7.4
ω_a(O4–H6)	3872.6	3693.7	3679.7	7.563	−32.4	−25.2	−11.2
ω_a(O1–H2)	3884.1	3710.6	3698.5	7.641	42.7	36.3	48.4
ω_a(O4–H5)	3872.6	3693.7	3679.7	7.563	76.1	69.0	83.0
	29.54	27.75	27.50		−0.38	−0.16	0.09
ZPE (kcal/mol)[b]	29.16	27.59	27.59				

[a] Bending force constants are given in (mdyn Å)/rad^2.
[b] ZPE values (second row) are given as the sum of the contribution of the local mode frequencies (first row, columns 2–4) and the contribution of the coupling frequencies (first row, columns 6–8).

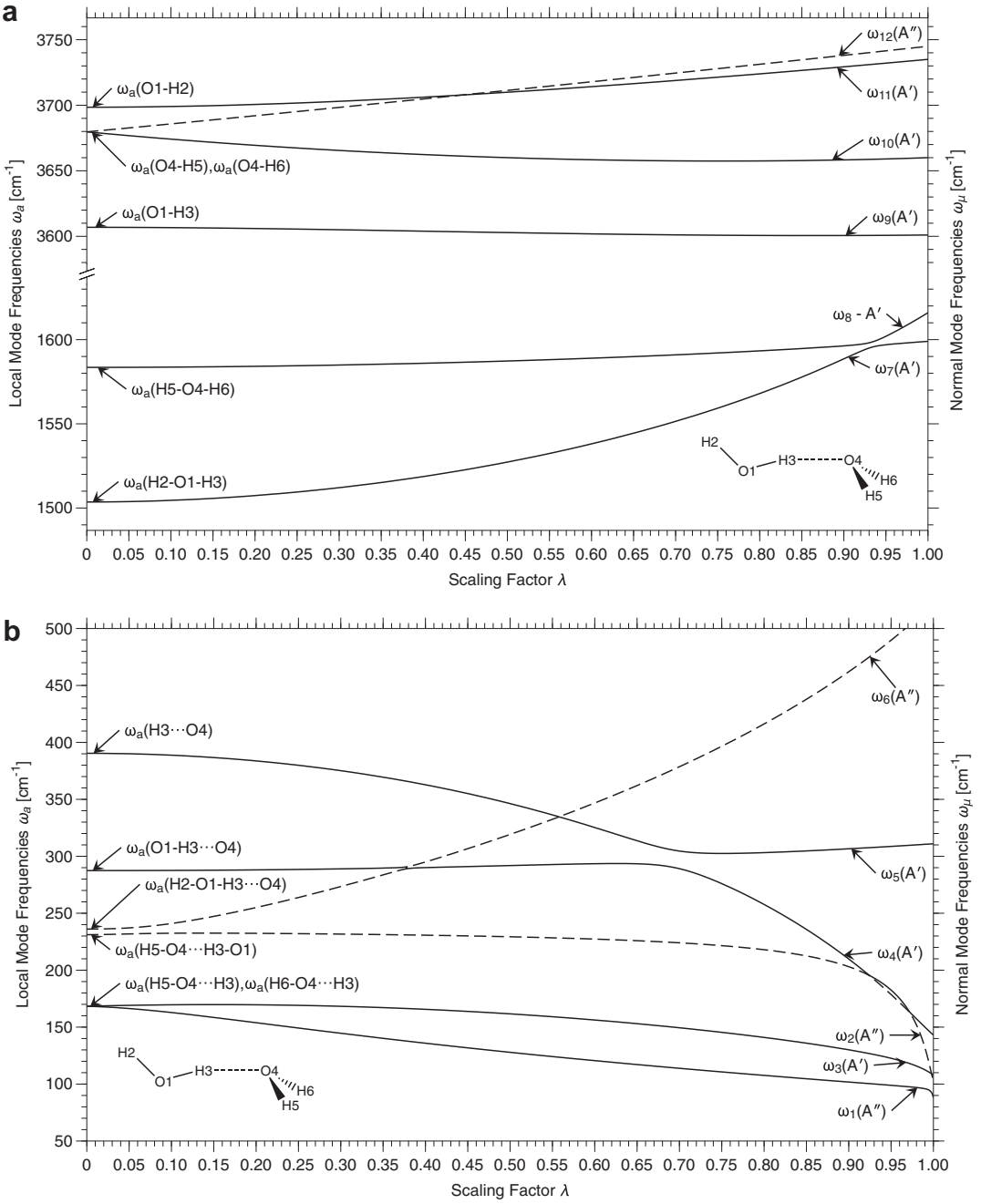

Figure 2. Adiabatic connection scheme relating experimental local mode frequencies (left) with experimental normal mode frequencies (right) of the water dimer. (a) Range from 1500 to 3800 cm^{-1}. (b) Range from 50 to 500 cm^{-1}. The adiabatic connection schemes for calculated harmonic frequencies are similar.

mode will be different for each H-bonded complex. This holds also for the normal mode frequency of the OH donor bond although anharmonicity and coupling effects are smaller in this case. A reliable account of the H-bond strength can only be provided by the local mode force constant $k_a = 0.085$ mdyn/Å (Table 3), which reveals that H-bonding is substantially stronger in **1** than suggested by a frequency value of 143^{-1}. This has been demonstrated by FKC [3].

Acknowledgement

This Letter was financially supported by the National Science Foundation, Grant CHE 1152357. We thank SMU for providing computational resources.

References

[1] G. Gilli, P. Gilli, The Nature of the Hydrogen Bond, IUCr Monographs on Crystallography, vol. 23, Oxford University Press, New York, 2009.
[2] Hydrogen bonding – new insights, in: S.J. Grabowski (Ed.), Challenges and Advances in Computational Chemistry and Physics, Springer, New York, 2006.
[3] M. Freindorf, E. Kraka, D. Cremer, Int. J. Quant. Chem. 112 (2012) 3174.
[4] Z. Konkoli, D. Cremer, Int. J. Quant. Chem. 67 (1998) 1.
[5] Y. Bouteiller, B. Tremblay, J.P. Perchard, Chem. Phys. 386 (2011) 29.
[6] A. Gutberlet, G. Schwaab, M. Havenith, J. Phys. Chem. A 115 (2011) 6297.
[7] K. Kuyanov-Prozument, M.Y. Choi, A.F. Vilesov, J. Chem. Phys. 132 (2010) 014304.
[8] C. Sandorfy, J. Mol. Struct. 790 (2006) 50.
[9] E.B. Wilson, J.C. Decius, P.C. Cross, Molecular Vibrations, McGraw-Hill, New York, 1955.
[10] W. Zou, R. Kalescky, E. Kraka, D. Cremer, J. Chem. Phys. 137 (2012) 084114.
[11] J. Decius, J. Chem. Phys. 38 (1963) 241.

[12] K. Raghavachari, G.W. Trucks, J.A. Pople, M. Head-Gordon, Chem. Phys. Lett. 157 (1989) 479.
[13] V. Barone, J. Chem. Phys. 122 (2005) 014108.
[14] H.G. Kjaergaard, A.L. Garden, G.M. Chaban, R.B. Gerber, D.A. Matthews, J.F. Stanton, J. Phys. Chem. A 112 (2008) 4324.
[15] D. Cremer, J.A. Larsson, E. Kraka, in: C. Parkanyi (Ed.), Theoretical and Computational Chemistry, vol. 5, Theoretical Organic Chemistry, Elsevier, Amsterdam, 1998, p. 259.
[16] Z. Konkoli, D. Cremer, Int. J. Quant. Chem. 67 (1998) 29.
[17] CFOUR, a quantum chemical program package written by J.F. Stanton, J. Gauss, M.E. Harding, P.G. Szalay with contributions from A.A. Auer, R.J. Bartlett, U. Benedikt, C. Berger, D.E. Bernholdt, Y.J. Bomble, O. Christiansen, M. Heckert, O. Heun, C. Huber, T.C. Jagau, D. Jonsson, J. Jusélius, K. Klein, W.J. Lauderdale, D.A. Matthews, T. Metzroth, D.P. O'Neill, D.R. Price, E. Prochnow, K. Ruud, F. Schiffmann, S. Stopkowicz, A. Tajti, J. Vázquez, F. Wang, J.D. Watts and the integral packages MOLECULE (J. Almlöf and P.R. Taylor), PROPS (P.R. Taylor), ABACUS (T. Helgaker, H.J. Aa. Jensen, P. Jørgensen, and J. Olsen), and ECP routines by A.V. Mitin and C. van Wüllen. For the current version, see http://www.cfour.de.
[18] S.K. Min, E.C. Lee, H.M. Lee, D.Y. Kim, D. Kim, K.S. Kim, J. Comput. Chem. 29 (2008) 1208.
[19] W. Klopper, J.G.C.M. van Duijneveldt-van de Rijdt, F.B. van Duijneveldt, PhysChemChemPhys 2 (2000) 2227.
[20] L.A. Curtiss, D.J. Frurip, M. Blander, J. Chem. Phys. 71 (1979) 2703.
[21] L.B. Braly, K. Liu, M.G. Brown, F.N. Keutsch, R.S. Fellers, R.J. Saykally, J. Chem. Phys. 112 (2000) 10314.
[22] F.N. Keutsch, L.B. Braly, M.G. Brown, H.A. Harker, P.B. Petersen, C. Leforestier, R.J. Saykally, J. Chem. Phys. 119 (2003) 8927.
[23] Y. Bouteiller, J.P. Perchard, Chem. Phys. 305 (2004) 1.
[24] U. Buck, F. Huisken, Chem. Rev. 100 (2000) 3863.
[25] Z.S. Huang, R.E. Miller, J. Chem. Phys. 91 (1989) 6613.